J. Phys. C: Solid State Phys. **21** (1988) 1691–1702. Printed in the UK

Monte Carlo simulations of excitation transfer in a randomly occupied cubic lattice

F Häring, E Müller, F Wünsch and W Gebhardt
Fakultät Physik, University of Regensburg, Regensburg, Federal Republic of Germany

Received 16 June 1987, in final form 15 September 1987

Abstract. Excitation transfer is considered in a randomly occupied FCC lattice. A model is constructed in which the excitation energy is assumed to be a stochastic variable. Transfer is only allowed between nearest neighbours. High excitation densities in the volume being considered are investigated. The results of computer simulations are compared with experiments on time-resolved emission spectroscopy in $Cd_{1-x}Mn_xTe$ and $Zn_{1-x}Mn_xTe$. It is found that all important properties of luminescence dynamics in these systems are well simulated by the present model.

1. Introduction

Transfer and trapping of optical excitations have been observed for many years. For incoherent energy transfer, several analytical approaches are available which give good results when periodic structures are considered and the approach is restricted to symmetrical transfer rates. In more general cases the analytical method is a formidable problem which can be solved only under severe restrictions. The consequences of these restrictions are not always obvious [1–10]. Therefore, several researchers have applied numerical methods [11–13], either to investigate the characteristics of a special model or to answer questions of energy transfer and trapping on specific lattices.

The computer simulations of the present work were motivated by measurements of photoluminescence in the dilute magnetic semiconductors $Cd_{1-x}Mn_xTe$ and $Zn_{1-x}Mn_xTe$ [14–17]. Time-resolved emission spectroscopy has been applied, and a variety of phenomena have been observed. In the FCC sublattices of the systems investigated, a fraction x of cations is replaced by transition-metal ions, typically Mn^{2+}. These ions act as donors in non-radiative energy transfer processes. The observed emission spectrum is a multiphonon sideband of the electronic transition $^4T_1 \rightarrow {}^6A_1$ which is additionally broadened by a wide distribution of transition energies. The reason for this is the random occupation of lattice sites by Mn^{2+} ions. Accordingly, each Mn^{2+} ion experiences a specific crystal field which depends on the environment and varies from site to site (figure 1). We, therefore, consider the excitation energy E as a stochastic variable. In our model, E is given by the number of nearest-neighbour donor sites. The radiationless energy transfer in manganese compounds is a consequence of the exchange interaction between Mn^{2+} ions. This interaction is short ranged, and we therefore restrict our considerations to transfer processes between nearest neighbours. Since the energy varies randomly, there is in general no energy resonance. This makes the transfer rather

0022-3719/88/081691 + 12 $02.50

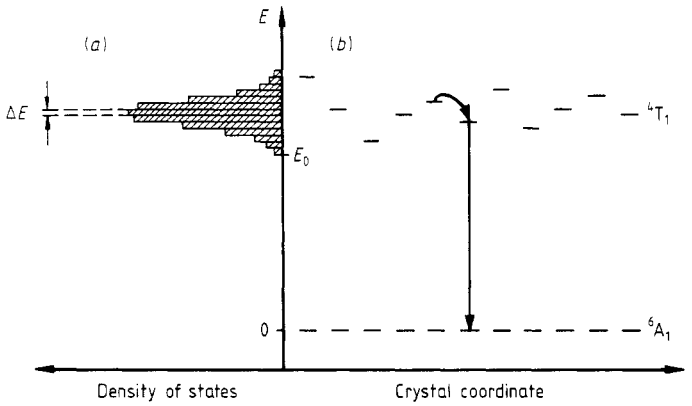

Figure 1. (*a*) The density of states Z_E leads to an inhomogeneous line broadening of the luminescence; (*b*) in the present model the excited-state energy E of the donor ions is a random variable which varies with the crystal coordinate.

slow, i.e. the transfer time is of the same order of magnitude as the radiative lifetime and lies in the microsecond range. The computer simulations enable us to answer the following questions. How does the spectrum change during excitation? How does it change in the dark period after excitation? What is the decay characteristic of the luminescence at a specific spectral energy? What is the decay law of the total emission? How does rise and decay change under a high excitation power?

In this paper, the model and the Monte Carlo (MC) technique are described in § 2. The results are presented in § 3. A discussion of the MC results is given in § 4, where a comparison with experimental results of photoluminescence measurements on $Cd_{1-x}Mn_xTe$ and $Zn_{1-x}Mn_xTe$ is also made. The summary and conclusion follow in § 5.

2. The model and the MC technique

2.1. The model

$Cd_{1-x}Mn_xTe$ and $Zn_{1-x}Mn_xTe$ crystallise in the zincblende structure. Since we are here concerned with radiationless excitation transfer between Mn^{2+} ions, we only have to consider the FCC sublattice of cations. We started the computer simulation with the construction of an FCC lattice with 16^3 lattice points and periodic boundary conditions. Each lattice point is considered as occupied with the probability x by an active ion or empty with probability $1 - x$. It is convenient to introduce a state variable attributed to each lattice point which can accept three values: -1 (empty); 0 (occupied and in the ground state); $+1$ (occupied and excited). The configurations of the total system are built up from all possible states of all lattice points. The energy E of the excited state changes with the local environment. We assume in a very simple approximation that the stochastic variable E depends linearly on the number n of occupied neighbouring sites:

$$E_n = E_0 + n\,\Delta E. \tag{1}$$

In this model the excited state of the Mn^{2+} ion accepts the lowest value if all neighbouring sites are empty. This assumption is quite well supported by luminescence experiments

using crystals with low manganese concentrations. The fraction of occupied lattice sites which have n occupied neighbouring sites is given by the binomial distribution

$$Z(x, n) = \binom{12}{n} x^n (1 - x)^{12-n}. \tag{2}$$

Since n is related to E by equation (1), we may also write

$$Z(x, n) = Z(x, E_n).$$

Then $Z(x, E_n)$ is the probability of finding occupied sites with energy E_n when the fraction x of all sites is occupied. The width of the distribution $Z(x, E)$ gives the inhomogeneous broadening of the expected luminescence.

2.2. *Excitation of active ions*

The number of photons with energy E absorbed per second is proportional to the absorption coefficient $\alpha(E)$ and the intensity $\mathcal{P}(E, t)$ of the exciting light

$$-\mathrm{d}N_{\mathrm{abs}}/\mathrm{d}t = C\mathcal{P}(E, t)\alpha(E) \tag{3}$$

where C is a constant of proportionality:

$$C = V_0/h\nu. \tag{4}$$

It contains the cell volume V_0 and the energy $h\nu$ of the absorbed photons. When excitation occurs with a short light pulse, $\mathcal{P}(E, t)$ may be replaced by

$$\mathcal{P}(E, t) = \mathcal{P}(E)\delta(t). \tag{5}$$

Then the number of excitations immediately after the pulse is

$$\Delta N_{\mathrm{abs}} = C\mathcal{P}(E)\alpha(E). \tag{6}$$

For the purpose of computer simulation, we use the following expression:

$$\Delta N_{\mathrm{abs}} = AP(E) \sum_{n=1}^{12} Z(x, E_n) G(E - E_n). \tag{7}$$

A is a constant and contains the probability for the transition $^6\mathrm{A}_1 \rightarrow {}^4\mathrm{T}_1$. $P(E)$ is the number of excitations created with energy E and $G(E - E_n)$ describes the absorption profile. E_n is the energy of the zero-phonon line as given by equation (1). The absorption profile may well be approximated by a Gaussian

$$G(E - E_n) = [1/\sigma(2\pi)^{1/2}] \exp[-(E - E_n - \Delta/2)^2]/2\sigma^2. \tag{8}$$

Δ is the Stokes shift between absorption and emission and σ^2 the second moment of the absorption band.

The computer simulation of excitation at energy E proceeds as follows.

(i) An occupied lattice site with energy E_n is selected at random.
(ii) A random number ν with $0 \leqslant \nu \leqslant 1$ is created.
(iii) $G(E - E_n)$ is determined.

If $G(E - E_n) > \nu$, the lattice site is considered to be excited. Otherwise a new occupied site is chosen and the procedure starts again. It is repeated P times when excitation by $P(E)$ incident photons are to be simulated. In the systems considered here,

excitations of multiphonon states are followed by fast relaxation processes. Therefore, as far as energy transfer processes are concerned, only the 'zero-phonon states' E_n are involved.

2.3. Excitation transfer

We now consider a lattice with only one excited lattice site which was prepared by the procedure described above. The excitation transfer will be restricted to hopping between nearest neighbours. We denote by i and j two neighbouring occupied lattice sites with energies E_i and E_j. If site i or j is excited, transfer occurs with the probabiltiies $w_{i\to j}$ or $w_{j\to i}$, respectively. The following relation holds:

$$w_{j\to i}/w_{i\to j} = \exp[-(E_i - E_j)/k_B T] \tag{9}$$

for $E_i \geqslant E_j$.

This assumption guarantees an equilibrium distribution and is equivalent to the condition of detailed balance. The following algorithm was used to simulate the hopping process.

(i) Assume that the excitation is at site $i = 0$; then transfer rates T_j are defined. If $j = 0$, the excitation stays at site $i = 0$. If $0 < j \leqslant 12$, transfer occurs to one of the 12 neighbours with the rate

$$T_j = \begin{cases} 0 & \text{site } j \text{ is empty} \\ 1 & \text{site } j \text{ is occupied and } E_0 \geqslant E_j \\ \exp[-(E_j - E_0)/k_B T] & \text{site } j \text{ is occupied and } E_0 \leqslant E_j. \end{cases} \tag{10}$$

(ii) A random number ν is chosen with $0 \leqslant \nu \leqslant \theta$. θ is given by the sum of all rates:

$$\theta = \sum_{j=0}^{12} T_j. \tag{11}$$

If

$$\nu \leqslant \sum_{j=0}^{k} T_j \tag{12}$$

transfer to the site k occurs.

The cycle just described is called a MC step and defines the time unit of the transfer process.

2.4. Bi-excitonic decay

It was observed in luminescence experiments that the intensity of the 2 eV luminescence in $Cd_{1-x}Mn_xTe$ shows a non-linear dependence on excitation power. This was interpreted by assuming an interaction between excited Mn^{2+} ions which leads to a non-radiative bi-excitonic decay. To simulate this bi-excitonic decay process we made an additional assumption.

If two neighbouring lattice sites are in the excited state, they undergo a non-radiative decay with a probability of unity. The decay process is assumed to be extremely fast.

Then in each MC step it is checked whether two neighbouring occupied lattice sites are simultaneously excited. If this is the case, both sites immediately undergo a transition into the ground state [18].

2.5. The time-resolved emission spectrum

In the general case we have to consider non-radiative transfer, radiative decay and bi-excitonic decay. We proceed in the following way to obtain the time-resolved emission spectrum $I(E, t_n)$ at time t_n. An FCC lattice is constructed using the procedure described in § 2.1. Each lattice site is either in the empty or in the occupied state. We create with each MC step $P(t_i)$ new excitations on occupied lattice sites according to § 2.2. We check in each step for bi-excitonic decay; let all excited single lattice sites decay radiatively with the probability $1/\tau_R$ and record the energy E_n. This is done for a certain number of MC steps, typically 65. The procedure is repeated as often as necessary to make the deviation from the average smaller than a given value. The histogram thus obtained is proportional to the emission spectrum $I(E_n, t_j)$. It is in practice much simpler to take care of the radiative decay by an exponential factor $\exp[-(t_j - t_i)/\tau_R]$. In this way, it does not have to be included in the simulation procedure. Then $I(E_n, t_j)\tau_R$ is simply the number of lattice sites with energy E_n excited at time t_j.

In the general case when bi-excitonic decay has to be considered, a complete MC simulation for an arbitrary excitation $P(t)$ is rather time consuming. The procedure is much simpler at low excitation densities. In this case the simulated spectrum does not depend on the excitation density. Let $\tilde{I}(E_n, t_j)$ be the luminescence spectrum obtained immediately after a δ-function-like excitation

$$P(t_j) = \delta(t - t_j).$$

Then the spectrum obtained with an arbitrary excitation $P(t_i)$ is

$$I(E_n, t_j) = \sum_{i=0}^{j} P(t_i)\tilde{I}(E, t_j - t_i) \exp\left(-\frac{t_j - t_i}{\tau_R}\right). \tag{13}$$

Since we have omitted phonon broadening, $I(E_n, t_j)$ must be considered as a zero-phonon spectrum with inhomogeneous broadening. Then, in analogy to equation (8), the luminescence band broadened by multiphonon processes is given by

$$I(E, t_j) = \sum_{n=0}^{12} I(E_n, t_j)A' \exp\left(\frac{(E - E_n - \Delta/2)^2}{2\sigma^2}\right). \tag{14}$$

In order to allow for a quantitative comparison with experiment, we calculated the zeroth, first and second moments of $I(E, t)$:

$$M_0 = I(t) = \int I(E, t)\,\mathrm{d}E \tag{15}$$

$$M_1 = \langle E \rangle = \frac{1}{M_0} \int E\, I(E, t)\,\mathrm{d}E \tag{16}$$

$$M_2 = \langle E^2 \rangle - \langle E \rangle^2 = \frac{1}{M_0} \int (E - \langle E \rangle)^2 I(E, t)\,\mathrm{d}E. \tag{17}$$

Note that all the three moments depend on time. This time dependence bears information on the distribution $Z(x, E)$ of excited states, on the excitation spectrum $G(E)$ and on the hopping dynamics which may be observed as a shift and a narrowing of the luminescence band.

For all MC simulations a computer of type VAX 11/750 at the University of Regensburg computer centre was used. The time which was necessary for the simulation of exciton transfer as described above was typically 17 CPU min, for bi-excitonic decay 90 CPU min and for trapping 30 CPU min.

2.6. Trapping

If the radiative lifetime τ_R is very long compared with the typical nearest-neighbour transfer time, the excitation visits a large number of active lattice sites. In this case the decay is in practice dominated by trapping. The present model may give at least a qualitative description of the decay even when the specific trapping mechanism is not well known.

We follow the random walk of the excitation through the FCC lattice on occupied lattice sites. It is then easy to obtain the number of lattice points R_j visited after j steps [12, 13, 19]. The first and the second moments of R_j, given by

$$S_j = \langle R_j \rangle \tag{18}$$

and

$$\sigma_j = \langle R_j^2 \rangle - \langle R_j \rangle^2 \tag{19}$$

respectively, determine approximately the decay of the luminescence intensity by trapping processes after j steps:

$$I_j \sim \exp(-\lambda S_j + \lambda^2 \sigma_j^2/2) \tag{20}$$

where λ depends on the concentration c of traps in the following way:

$$\lambda = -\ln(1 - c). \tag{21}$$

Unfortunately the experimental situation of trapping in $Cd_{1-x}Mn_xTe$, $Zn_{1-x}Mn_xTe$ and related systems is rather complex and not well defined [16, 17]. We therefore do not follow this discussion further but refer to recent publications [20–22].

3. Results of MC simulations

3.1. Low excitation densities at low temperatures

We consider the following experimental situation. The luminescence is excited on the high-energy side of the absorption with a laser in continuous-wave operation (see figure 1). After a steady state condition is reached, the laser is turned off. Three spectra are recorded. The first is taken immediately after the laser is switched on, the second shortly before the laser is switched off and a third is taken in the dark period. The crystal temperature is kept low, i.e.

$$k_B T \ll \Delta E.$$

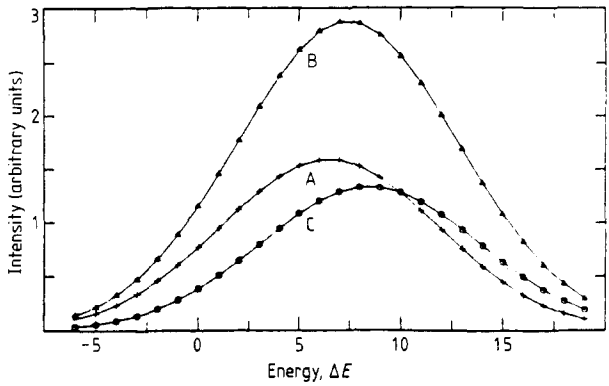

Figure 2. Three spectra obtained after a rectangular 'pulse excitation' at $E = E_0 + 12\,\Delta E$ with $\sigma = 7\Delta E$ (equation (8)): A, taken immediately after starting the excitation; B, taken shortly before the excitation is turned off after a steady state was reached; C, taken shortly after the excitation is turned off.

Figure 2 shows a plot of the three simulated spectra broadened by phonons. The intensity increases during excitation and shifts to lower energies. In the dark period the intensity decays and the band is shifted further to lower energies. Furthermore a broadening is observed during excitation. The variation in band position and width with time is seen better in figure 3, where the first and second moments are plotted. The first moment or centre of mass of the luminescence band decreases continuously with increasing time. The second moment which is proportional to the square of half-width increases during excitation but decreases again after the light is switched off.

3.2. Low excitation densities at high temperatures

The temperature dependence arises from the definition of transfer probabilities as given by equation (9). In figure 4 the total shift of the first moment during decay is plotted against temperature (see upper curve). A decrease in the shift with increasing temperature is observed.

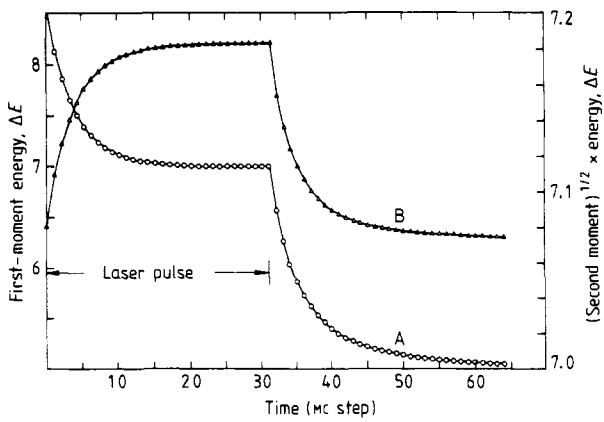

Figure 3. The first (curve A) and second (curve B) moments of spectra excited as in figure 2 plotted as a function of time measured in MC steps.

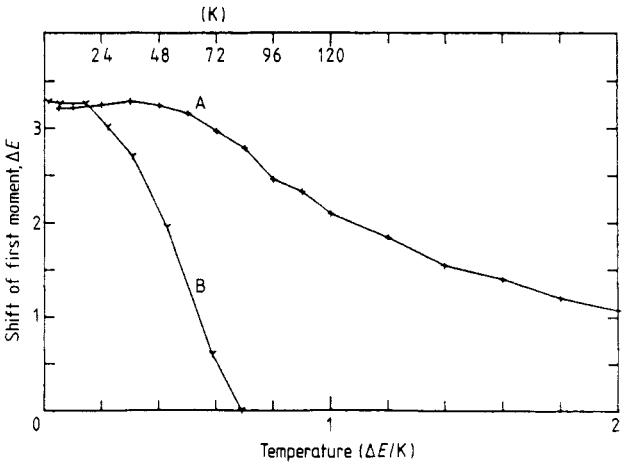

Figure 4. The total shift of the first moment with temperature: curve A, MC simulation; curve B, experimental results for $Cd_{0.35}Mn_{0.65}Te$. Note that the MC simulations were continued until the band position remained constant, whereas the experimental points were taken after a finite time interval (64 μs).

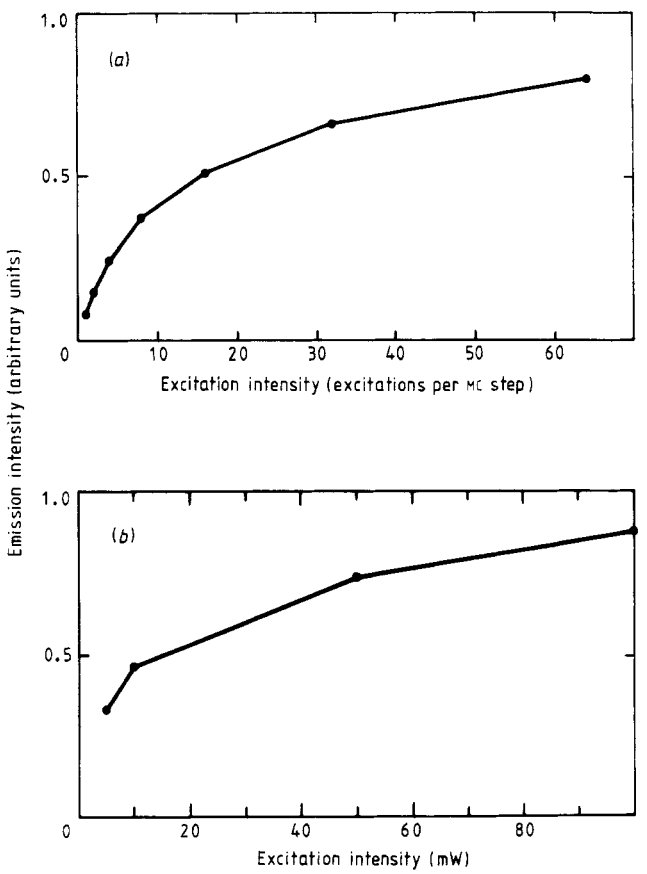

Figure 5. Non-linear relationship between the intensity of luminescence and excitation power at high levels of excitation: (*a*) simulated values plotted against excitations per MC step; (*b*) experimental points for $Cd_{0.35}Mn_{0.65}Te$.

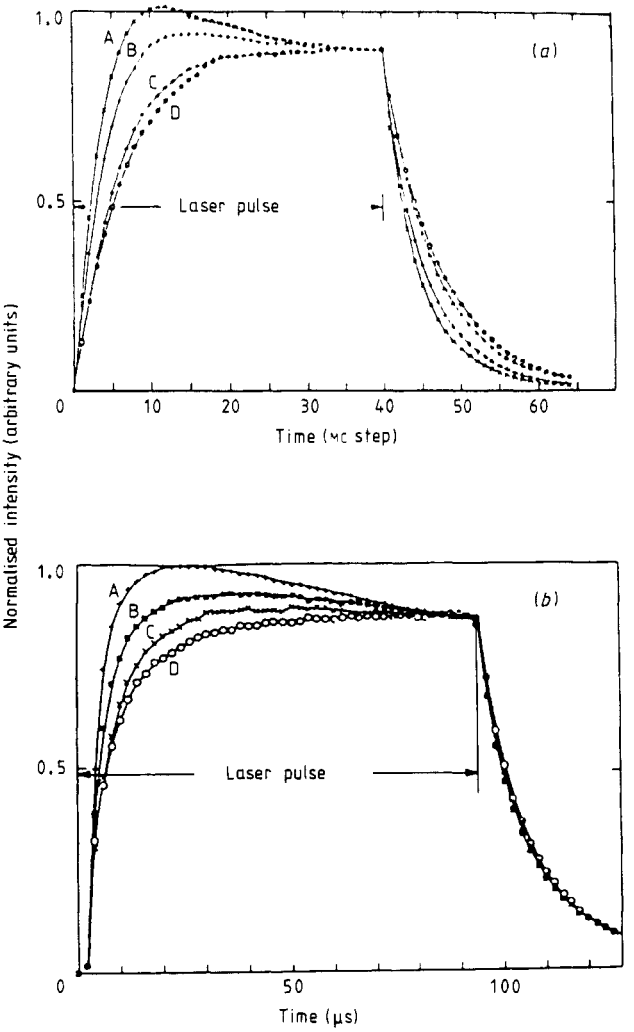

Figure 6. Simulated dynamics of the luminescence on the high-energy side of the band and at various excitation levels: (*a*) MC simulation (curves: A, 100 excitations per MC step; B, 50 excitations per MC step; C, 10 excitations per MC step; D, 5 excitations per MC step); (*b*) experimental results on the 5700–6108 emission for $Cd_{0.35}Mn_{0.65}$ (curves: A, 100 mW; B, 50 mW; C, 10 mW; D, 5 mW).

3.3. High excitation densities

At high excitation densities the excitation transfer is dominated by bi-excitonic effects. Therefore the integrated emission intensity deviates from a linear relationship and approaches saturation (figure 5(*a*)). The increase in emission intensity during excitation shows a characteristic change with excitation power. In figure 6(*a*) the emission at the high-energy wing of the luminescence band is plotted against time. The two upper curves, taken at high excitation power, show an increase until a maximum is reached; then the intensity decreases and approaches a steady value. This overshooting is not observed for the low-energy wing.

4. Comparison with luminescence experiments on $Cd_{1-x}Mn_xTe$ and discussion

The dynamics of the first and second moments determined from low-temperature luminescence experiments on $Cd_{0.35}Mn_{0.65}Te$ are shown in figure 7. The experimental curves are qualitatively very similar to the simulated curves and show all the characteristic features mentioned in § 3.1. Fairly good quantitative agreement with experimental results is achieved with the choice

$$\Delta E = 10 \text{ meV}.$$

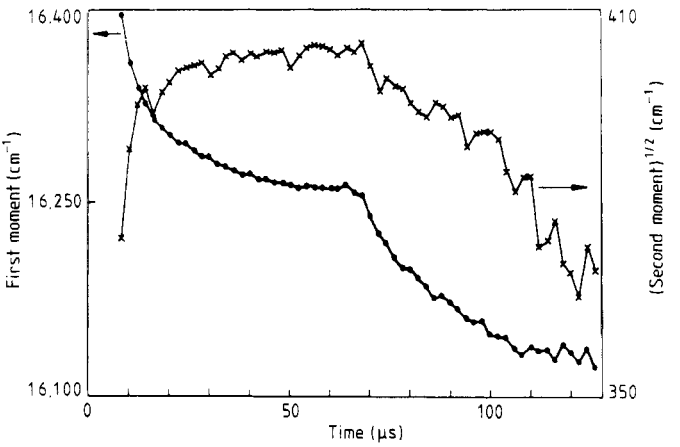

Figure 7. Experimental data of first (curve A) and second (curve B) moments of the luminescence band in $Cd_{0.35}Mn_{0.65}Te$ at 2.2 K.

The phenomena shown in figures 2, 3 and 7 are obviously the result of excitation on the high-energy side of the inhomogeneously broadened absorption (see figure 1) and of slow hopping transfer to lower-lying levels during the radiative lifetime.

Figure 6(*b*) shows experimental results at a high excitation power. The qualitative behaviour of the increase is well simulated by the MC calculation (see figure 6(*a*)). The normalised experimental decay curves almost coincide, whereas the calculated decay shows some dependence on the excitation power. The reason for this disagreement is not yet understood.

Reasonable quantitative agreement of the data in figures 5 and 6 is reached when the experimental results obtained with a 100 mW laser beam are compared with MC simulation of 100 excitations per MC step. The radiative lifetime was simulated by setting τ_R equal to 6.6 MC steps. A typical τ_R value is about 20 μs which leads to a transfer time τ(MC) of 3 μs. A simulated 16^3 lattice with $x = 0.65$ has 2662 active lattice sites. With 100 excitations per MC step, their excitation probability would then be 25% if bi-excitonic decay is neglected. We obtain another estimate of the excitation density from the experimental conditions by considering the focal diameter of the laser beam, and the absorption and reflection losses. Without bi-excitonic decay, this gives an excitation probability of 15% in the stationary state, which is in reasonably good agreement with the MC simulations and corresponds to an excitation density N_1 of 3×10^{26} m^{-3}. The real

excitation density N_2 can be estimated with regard to bi-excitonic decay. A fit of the experimental data (see figure 5(*b*)) gives

$$N_2 = 0.2\,N_1$$

with an excitation power of 100 mW. With this ratio the rate equation

$$\dot{N}_2 = -k_R N_2 - k_2 N_2^2 + \mathcal{P} \tag{22}$$

can be solved for the stationary state

$$\dot{N}_2 = 0.$$

We obtain a value for the bi-excitonic decay constant as follows:

$$k_2 = 3.5 \times 10^{-13}\ \mathrm{m^3\ s^{-1}}.$$

The temperature dependence of energy transport is usually a critical test of the used model. In the present case, unfortunately, the model fails to give the correct temperature dependence (figure 4). The measured shift of the first moment decreases rapidly with increasing temperature, whereas the simulated temperature dependence is much weaker. In comparing the two curves in figure 4, we should first comment on the experimental conditions. The luminescence intensity was only observed during a limited time interval, typically $3\bar{\tau}$, where $\bar{\tau}$ is the average decay time [17]. However, at $t = 3\bar{\tau}$, steady state is not yet reached, but the first moment seems still to decrease somewhat when $t > 3\bar{\tau}$. The simulated moments, however, were taken at steady state conditions. Accordingly the experimental points have to be considered as a lower limit of the energy shift. However, this accounts for only a part of the discrepancy.

It is well known that $Cd_{1-x}Mn_xTe$ and $Zn_{1-x}Mn_xTe$ exhibit spin-glass properties if the manganese concentration exceeds the percolation limit $x = 0.17$. The spin of the active ions has therefore to be considered as an additional random variable. In this case, both the excitation energy and the transfer rate become spin dependent. It is then reasonable to consider the variable part of the excitation energy $n\,\Delta E$ to consist of a spin-dependent and a spin-independent (Coulomb or elastic) contribution. The experiments suggest that the spin-dependent splitting has vanished at temperatures higher than 65 K [16, 17]. The simulation of the spin configuration is in itself a difficult problem in which one has to take into account the spin-glass properties of the material [20]. This was not attempted in the present work.

5. Summary and conclusion

Energy transfer processes were simulated in a randomly occupied FCC lattice with nearest-neighbour transfer. The excited-state energy is considered to be a random variable. The transfer rates are chosen so as to guarantee a detailed balance.

A MC procedure was used to study the following processes:

(i) donor–donor transfer and radiative decay at low excitation level and various temperatures;

(ii) donor–donor transfer, radiative decay and bi-excitonic decay at a high excitation level and low temperatures.

The MC simulations were motivated by time-resolved measurements of the photoluminescence in $Cd_{1-x}Mn_xTe$ and $Zn_{1-x}Mn_xTe$. In these compounds the cation sites are

randomly occupied by Mn^{2+} ions, which form the donors of the energy transfer processes. The random variable E reflects the varying crystal field.

A comparison of the results from computer simulations with those from time-resolved luminescence measurements shows that all important properties of the investigated systems can be simulated with the proposed model. However, the model fails to give a realistic temperature dependence. The reason is to be found in a further complication of the real systems, in which at low temperatures the exchange interaction between the Mn^{2+} ions contributes to the energy difference and to the transfer rate between neighbouring ions.

References

[1] Lyo S K, Holstein T and Orbach R 1978 *Phys. Rev.* B **18** 1637
[2] Huber D L 1979 *Phys. Rev.* B **20** 5333
[3] Huber D L 1979 *Phys. Rev.* B **20** 2307
[4] Huber D L 1985 *International School of Physics Enrico Fermi, Summer Courses*
[5] Burshtein A J 1985 *J. Lumin.* **34** 167
[6] Watts R K 1975 *Proc. Nato Advanced Study Inst. (Erice) 1974* Series B, vol 8, ed. B di Bartolo, p 307
[7] Blumen A, Klafter J and Silbey R 1980 *J. Chem. Phys.* **72** 5320
[8] Blumen A and Zumofen G 1980 *Chem. Phys. Lett.* **70** 387
[9] Zumofen G and Blumen A 1982 *Chem. Phys. Lett.* **88** 63
[10] Zumofen G and Blumen A 1982 *J. Chem. Phys.* **76** 3713
[11] Zumofen G and Blumen A 1981 *Chem. Phys. Lett.* **78** 131
[12] Blumen A and Zumofen G 1981 *J. Lumin.* **24–25** 781
[13] Klafter J, Zumofen G and Blumen A 1982 *J. Physique Lett.* **45** L49
[14] Müller E, Gebhardt W and Gerhardt V 1982 *Phys. Status Solidi* b **113** 209
[15] Müller E and Gebhardt W 1984 *J. Lumin.* **31–32** 479
[16] Müller E 1986 *Dissertation* Regensburg
[17] Müller E and Gebhardt W 1986 *Phys. Status Solidi* b **137** 259
[18] Strauss E, Maniscalco W J, Yen W M, Kellner V C and Gerhardt V 1978 *Phys. Rev. Lett.* **44** 824
[19] Klafter J 1985 *International School of Physics Enrico Fermi, Summer Courses*
[20] Goede O and Dang Dinh Thong 1984 *Phys. Status Solidi* b **124** 343
[21] Ehrlich Ch, Busse W, Gumlich H-E and Tschierse D 1985 *J. Cryst. Growth* **72** 371
[22] Tschierse D 1986 *Dissertation* Berlin
[23] Kett H, Gebhardt W and Krey U 1984 *J. Magn. Magn. Mater.* **46** 5–10